Chapter 5: Boundary-condition problems in two and three dimensions: Cartesian coordinates (04 Oct 2021).

A. Perspective and summary.

In boundary-condition (boundary-value) problems the potential or electric field is specified on a surface *S* that completely encloses a volume of interest *V*, which may or may not contain a charge density ρ. The objective is to determine $\phi(\vec{r})$ everywhere within *V*.

We derived the formal solution of Poisson's Equation and discussed some general properties in Ch. 4. In Chs. 5, 6, and 7 these methods and others are put to use, being applied to configurations whose surfaces are defined by the condition (coordinate = constant), examples of which are shown below. Chapter 5 deals with Cartesian coordinates, with configurations consisting of infinite planes and rectilinear shapes such as blocks and cubes. This is the logical place to start, because solutions involve functions that are now second nature to all of us: real and complex exponentials, and their linear combinations: sines, cosines, and their hyperbolic equivalents. This allows us to focus on the methods, not the functions. Our primary goal here is not to obtain the solutions, but to understand the different methods by which these solutions are obtained. Consider Indo-European languages as a parallel: the words (orthogonal functions) change, but the subject-verb-predicate structure (methods) remains the same.

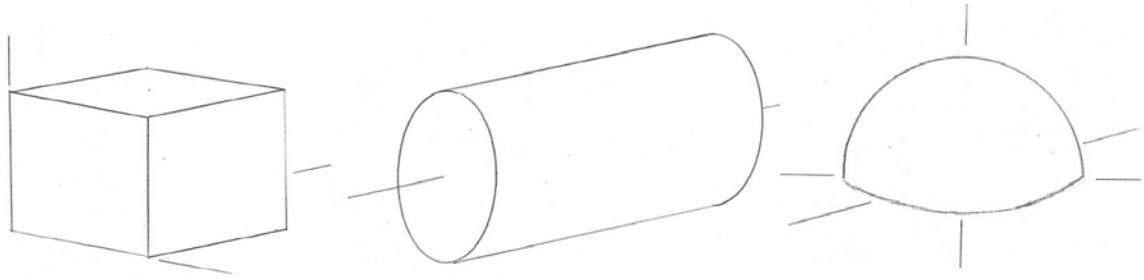

After the methods have become familiar, objects based on cylindrical shapes are considered in Ch. 6. Here, constant-coordinate surfaces include not only cylinders but

also wedges. The mathematical treatments of these objects are more interesting than Cartesian treatments in part because the Laplacian in cylindrical coordinates forces interconnections among the eigenfunctions that have no parallel in the Cartesian system. The collection of eigenfunctions now includes Bessel functions as well as monomials ρ^{in} raised to complex powers. An image-line-charge analog of the Cartesian image-charge configuration is discussed, although the mathematics is significantly more complicated. For spherical coordinates, a complete development of (coordinate = constant) objects based on spherical coordinates is considerably more exotic (think Bessel functions of imaginary order), so in Ch. 7 we follow the usual convention of restricting attention to the lightling rod and objects with spherical symmetry, such as the spherical shell. As you work through this collection of functions, keep in mind that, whatever the mathematics, the procedures remain the same.

From a mathematical perspective, except for image-charge applications Chs. 5, 6, and 7 are based on only three equations: Laplace's Equation

$$\nabla^2\phi(\vec{r}) = 0\,; \tag{5.1}$$

the Green-function equation:

$$\nabla^2_{\vec{r}'}G(\vec{r},\vec{r}') = -4\pi\delta(\vec{r}-\vec{r}')\,; \tag{5.2}$$

and Green's Theorem:

$$\phi(\vec{r}) = \int_V d^3r'\,\rho(\vec{r}')G(\vec{r},\vec{r}') - \frac{1}{4\pi}\int_S d^2r'\left(\phi(\vec{r}')\frac{\partial G(\vec{r},\vec{r}')}{\partial n'} - G(\vec{r},\vec{r}')\frac{\partial\phi(\vec{r}')}{\partial n'}\right). \tag{5.3}$$

Superposition remains a fundamental principle, and for series solutions, orthogonal functions complete the picture.

The solutions $\phi(\vec{r})$ themselves fall into four categories of increasing computational difficulty:

(1) image-charge solutions, which are either analytic or can be represented as integrals;
(2) series expansions of $\phi(\vec{r})$ in orthogonal and related functions, where each term is a solution of Laplace's Equation;
(3) series expansions of $G(\vec{r},\vec{r}')$ in orthogonal and related functions, where each term is a solution of Laplace's Equation; and
(4) series expansions of $G(\vec{r},\vec{r}')$ in orthogonal functions.

Analytic solutions are clearly preferred, but with very few exceptions, image-charge solutions exist only for the infinite plane, two-dimensional regions of circular cross section (Ch. 6), and the spherical shell (Ch. 7). Note that the infinite-plane configuration is a special case of the spherical shell.

The inapplicability of the image-charge method means that most boundary-condition problems are solved by series expansions. For configurations defined by (coordinate = constant), these in turn are based on polynomials that are orthogonal in the coordinate system appropriate to the configuration. These expansions are obtained by the following steps:

(1) Identify the coordinate system describing the configuration;

(2) List the eigenfunctions and eigenvalues of the appropriate Laplacian, separating them according to whether they have positive and negative curvature, i.e., are monatonic or oscillatory, respectively;

(3) For the facet of current interest, select the eigenfunctions that form a complete set for expanding the potential over the facet, and hence form the basis of a series solution;

(4) Determine the eigenvalues of these eigenfunctions by requiring that the expansion terms be zero at all other boundaries;

(5) Use orthogonality to determine the coefficients of the terms of the series.

Note that condition (4) serves a secondary purpose: by requiring expansions to be zero on all other facets, it ensures that the solutions are independent. Since the equations are linear, the complete solution for the object is then the sum of the solutions for its individual facets. If a charge density is present in the object, then Green-function methods are required. We consider mainly Dirichlet Green functions, where parameters must be chosen such that the terms of the series are zero on all surfaces.

The chapter evolves along the route of increasing complexity. Section B begins with the image-charge determination of the analytic Dirichlet and Neumann Green functions for a conductor at zero potential filling the half-space $z \le 0$. By converting the Dirichlet solution to its empty-space equivalent using real charges (q and the induced surface charge density) as opposed to the virtual image charge, we obtain insights into Green functions that are not evident from mathematics alone. Section C shows that these insights allow us to solve the problem of determining the current density in a conductor in the half-space $z \le 0$ that results from a charge q moving with a velocity $\vec{v}$ parallel to its surface.

In Sec. D we evaluate $\phi(\vec{r})$ for configuration where the potential is defined in the $z = 0$ plane. Building on Sec. C, in Sec. E we consider a simple configuration, the disc of radius a, from Dirichlet, Neumann, and free-space perspectives, again to get a better idea of the physics described by the different approaches.

Series solutions begin in Sec. F with the cube, an obvious choice because the associated functions are familiar. Taking advantage of the experience gained with Fourier expansions, in Sec. G we investigate the Fourier representation of the free-space Green function, then return to series expansions for Green functions of the $z = 0$ plane. Sections H and I treat two-dimensional configurations, including an introduction to conformal mapping.

I had originally intended this chapter to supplement both Jackson's Chs. 2 and 3, but there is enough material here to require three chapters. Jackson says relatively little about planar configurations, covering the image-charge configuration in Sec. 2.1, the cube in Sec. 2.9, and a two-dimensional example in Sec. 2.10. The second edition covers conformal mapping, but in the third edition this section was replaced by one on finite-element analysis. Nearly all of Jackson's Chs. 2 and 3 is devoted to the mathematics of spherical coordinates, which we cover in abbreviated form in Ch. 7. We give more emphasis to cylindrical than spherical coordinates, mainly because these provide a better

example of interconnected functions than does the spherical case. These interconnections are what distinguishes eigenfunctions in cylindrical and spherical coordinates from those of Cartesian coordinates, thereby providing additional justification for putting them in separate chapters.

B. Image-charge solutions: Green functions of the conducting plane.

As noted in the previous section, a major advantage of image-charge solutions is that they provide results that are either analytic or can be expressed as integrals. In its most basic form, in the image-charge philosophy we replace the configuration that we cannot solve with a configuration that we can, with the restriction that all conditions match at the boundary. We then retain that part of the solution that overlaps the volume of interest, and discard the rest.

A second major advantage is that the Dirichlet Green function of a configuration follows immediately from the solution for $\phi(\vec{r})$ for a point charge q located at $\vec{r}_o$ with all boundaries at zero potential. In this case $\phi(\vec{r})$ is given by

$$\nabla^2\phi(r) = -4\pi\rho(\vec{r}) = -4\pi q\delta(\vec{r}-\vec{r}_o)\,, \tag{5.4}$$

with $\phi(\vec{r}_s) = 0$. A comparison of Eqs. (5.4) and Eq. (5.2) shows that the Dirichlet Green function $G_D(\vec{r},\vec{r}\,') = \phi(\vec{r})$ with $q = 1$ and $\vec{r}\,' = \vec{r}_o$. This is what we expect for linear systems, with the volume term in Eq. (5.3) representing the superposition limit.

In the classic image-charge configuration, a point charge q is located on the z axis at a distance d from a grounded conductor filling the half-space $z \le 0$, as shown in the figure. The volume of interest is the space $z \ge 0$, which is enclosed by the $z = 0$ plane and the hemisphere of infinite radius defined by $|\theta| \le \pi/2$. The configuration is a natural extension of what we covered in Ch. 4, and the solution is already familiar to everyone who took undergraduate E&M. The surrogate configuration consists of the charge q at $\vec{r}_q = \hat{z}d$ in the volume of interest, and a second charge $(-q)$ at the image point $\vec{r}_q\,' = -\hat{z}d$ outside the volume of interest.

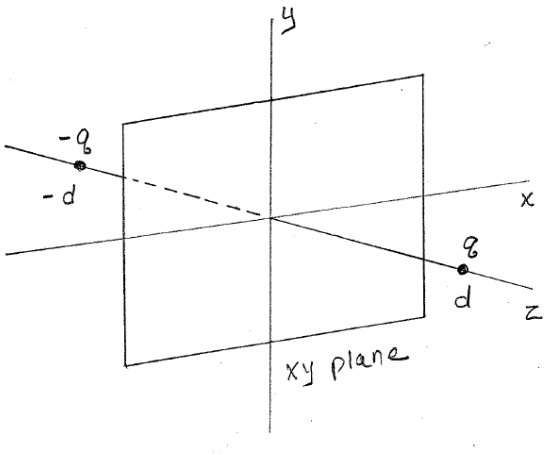

Considering q to be located at the more general point $\vec{r}_o = (x_o, y_o, z_o)$, $\phi(\vec{r})$ is given by

$$\phi(\vec{r}) = \frac{q}{|\vec{r}-\vec{r}_o|} - \frac{q}{|\vec{r}-\vec{r}_o\,'|} \tag{5.5a}$$

$$= \frac{q}{\sqrt{(x-x_o)^2+(y-y_o)^2+(z-z_o)^2}} - \frac{q}{\sqrt{(x-x_o)^2+(y-y_o)^2+(z+z_o)^2}}\,. \tag{5.5b}$$

$\phi(\vec{r})$ is zero at $z = 0$ and at infinity, and thereby not only satisfies Gauss' Equation but also the boundary conditions of the original configuration. Although Eqs. (5.5) are valid over all space, only the part $z \geq 0$ is relevant for the conductor filling the half-space $z \leq 0$. In this picture the image charge $(-q)$ assumes virtual, not real, status: it simulates the field generated by the surface charge density σ induced by *q* on the surface of the conductor. We follow up on this below.

From the above recipe the Dirichlet Green function of the configuration is

$$G_D(\vec{r},\vec{r}') = \frac{1}{\sqrt{(x-x')^2+(y-y')^2+(z-z')^2}} - \frac{1}{\sqrt{(x-x')^2+(y-y')^2+(z+z')^2}}. \tag{5.6}$$

Although Eq. (5.6) contains two singularities, only one is in the volume of interest and hence the appropriate Green-function conditions are satisfied. From the perspective of an observer in the volume of interest, $G_D(\vec{r},\vec{r}')$ automatically generates an image distribution $\rho'(\vec{r})$ for any $\rho(\vec{r})$ therein to ensure that the potential is equal to zero on the $z = 0$ plane. No additional input is required. This is one of the advantages of Green functions: the virtual charge distribution needed outside the volume of interest to realize the boundary condition $\phi(r) = 0$ on *S* is generated automatically.

The Neumann Green function for this configuration can also be constructed from the point-charge solution. $G_N(\vec{r},\vec{r}')$ is defined by $\nabla^2_{\vec{r}'} G_N(\vec{r},\vec{r}') = -4\pi\delta(\vec{r}-\vec{r}')$, but differs in that $\partial G_N/\partial n' = 4\pi/A_S = 0$ (zero follows because $A_S \to \infty$ for this configuration.) In the above the normal derivative is eliminated simply by changing the sign of the second term in Eq. (5.6). The result is

$$G_N(\vec{r},\vec{r}') = \frac{1}{\sqrt{(x-x')^2+(y-y')^2+(z-z')^2}} + \frac{1}{\sqrt{(x-x')^2+(y-y')^2+(z+z')^2}}, \tag{5.7}$$

This is equivalent to replacing the image charge $(-q)$ in Eq. (5.4) with $(+q)$. We return to the Neumann Green function below.

Having done the math, we now look at the physics. This is done by adopting the microscopic perspective, where the real charges of the configuration, *q* and the surface charge density σ induced by *q*, are assumed to be embedded in empty space. In this picture the image charge $(-q)$ is gone, replaced by $\sigma(x, y)$. Also, the Green function is no longer given by Eq. (5.6), but is now $G_D(\vec{r},\vec{r}') = |\vec{r}-\vec{r}'|^{-1}$, the Green function of empty space.

σ is calculated as usual by applying Gauss' Theorem to a small box straddling the interface and using the boundary condition that the field in the conductor is zero. For

mathematical simplicity we assume that q is located at $(0,0,d)$. From Eq. (5.5b) the field on the positive-z side is

$$\begin{aligned}\vec{E}(x,y,0) &= -\nabla\phi\big|_{z=0} \\ &= -\hat{z}\left(-\frac{1}{2}\frac{2q(z-d)}{(x^2+y^2+(z-d)^2)^{3/2}} - \frac{1}{2}\frac{2(-q)(z+d)}{(x^2+y^2+(z+d)^2)^{3/2}}\right)_{z=0} \\ &= -\hat{z}\frac{2qd}{\left(x^2+y^2+d^2\right)^{3/2}}, \end{aligned} \tag{5.7}$$

in which case

$$\sigma(x,y,0) = -\frac{1}{2\pi}\frac{qd}{(x^2+y^2+d^2)^{3/2}} \tag{5.8}$$

noting that for the Gaussian-box calculation $\hat{n} = \hat{z}$. The induced charge is negative, as expected, and has a distribution determined by its inability to escape from the conductor together with the competition between attraction to q and local in-plane Coulomb repulsion. As a cross-check, it is easily verified that the integral of Eq. (5.8) over the $z = 0$ plane is $(-q)$. σ is shown schematically in the figure.

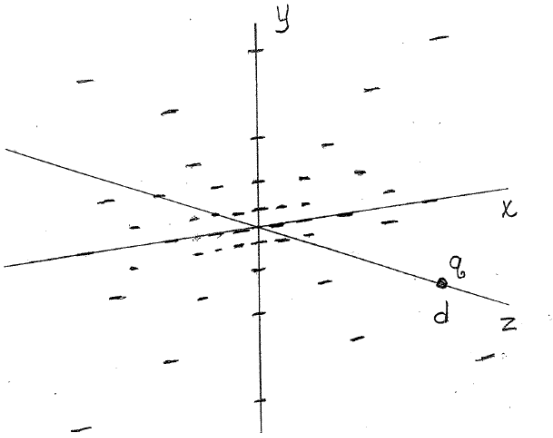

To proceed with the microscopic perspective, we next need the potential. This is given formally by the volume term in Eq. (5.3), where

$$\rho(\vec{r}\,') = q\delta(\vec{r}\,'-\hat{z}d) + \sigma(x',y',0)\delta(z'), \tag{5.9}$$

where $\sigma(x',y',0)$ is given by Eq. (5.8), and $G_D(\vec{r},\vec{r}\,')$ is the Green function of empty space. It follows that

$$\phi(\vec{r}) = \frac{q}{|\vec{r}-\vec{r}\,'|} - \frac{qd}{2\pi}\int_S dx'dy'\left(\frac{1}{(x'^2+y'^2+d^2)^{3/2}}\frac{1}{\sqrt{(x-x')^2+(y-y')^2+z^2}}\right). \tag{5.10}$$

Although the surface integral is formidable, we already know the answer for $z > 0$: its contribution is the same as that of an image charge $(-q)$ located at the image location $(-\hat{z}d)$. Noting that Eq. (5.8) is not changed when $z \to -z$, the solution for $z < 0$ is obviously that of an image charge $(-q)$ located at $\vec{r}_q = \hat{z}d$. But this is precisely what we could have predicted by symmetry; no math is required. Following through, for the observer at $z < 0$, $(-q)$ is superposed exactly on q, cancelling it out completely and thereby leaving no field inside what initially was the conductor. $\phi(\vec{r})$ is therefore given by

$$\phi(\vec{r}) = \text{Eq.(5b)} \quad \text{for } z > 0; \tag{5.11a}$$

$$= 0 \quad \text{for } z \le 0. \tag{5.11b}$$

The microscopic picture is a bit different: here, we superpose the *fields* of q and $(-q)$, so the cancellation occurs at the field rather than the charge level. Of course, the net result is the same.

Although we work here with a special configuration, this cancellation in conductors in the microscopic picture is general, and can be shown as follows. Consider a closed surface S inside a grounded conductor defining a volume of interest V described by a Dirichlet Green function $G_D(\vec{r},\vec{r}')$. Suppose that a charge density $\rho(\vec{r}')$ exists in V. With no field in the conductor itself, by Gauss' Theorem the screening charge density σ on S is

$$\sigma = -\frac{1}{4\pi}\hat{n}\cdot\nabla\phi,$$

where $\hat{n}$ points away from the volume of interest. But by construction of σ the field and therefore the potential are zero outside the volume of interest, hence the potential arising from σ cancels the potential from $\rho(\vec{r}')$ at everywhere outside S. Therefore, the proof of this proposition reduces to the question of whether such a solution for $\phi(r)$ exists. However, Green's Theorem is general, imposing no restrictions on $\rho(\vec{r}')$. Thus $\phi(\vec{r})$ exists, and so the cancellation is general.

Returning to the Neumann Green function, in the full-space perspective $G_D(\vec{r},\vec{r}')$ and $G_N(\vec{r},\vec{r}')$ lead to very different results for the same nominal configuration. This is discussed in Sec. D. In the next section we apply the Dirichlet result to a relevant problem that not usually considered in a course of graduate-level electrodynamics.

C. Image charges and superposition: currents induced in a conductor.

The problem considered is illustrated in the figure. A point charge q moves with a velocity $\vec{v} = v\hat{x}$ parallel to, and at a distance d above, the planar surface of a conductor of conductivity σ_c. If the conductor fills the half-space $z \le 0$, what is the current induced in the conductor?

We know from the previous section that in the electrostatics case this configuration can be treated by the image-charge method, with the result that the surface charge density σ induced on the surface of the conductor by q always looks like a point charge $(-q)$ located on the side opposite the observer. In the dynamic case, we expect that the same picture is approximately correct if v is slow

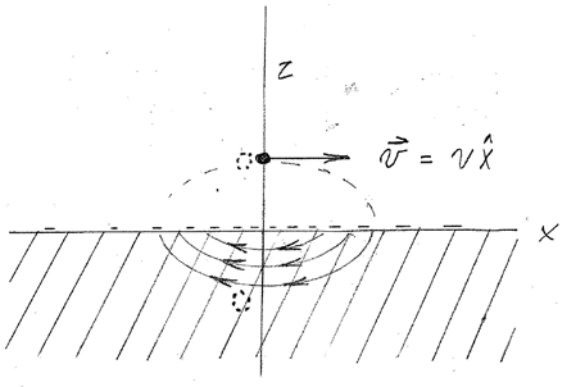

enough and the relaxation time of the free charge in the conductor is fast enough so that a quasi-equilibrium situation is maintained. In physical terms this means that any nonequilibrium charge distribution induced by *q* relaxes quickly on the laboratory time scale. From a previous homework problem, we calculated $\tau = \varepsilon/4\pi\sigma_c = \Delta t$ from Ampère's Equation. Substituting $\rho = 1.7\times10^{-8}\ \Omega\,\mathrm{m}$ for Cu and converting to conductivity in cgs units, we find $\sigma_c \simeq 5\times10^{17}\ \mathrm{s}^{-1}$. Therefore $\tau = \Delta t \simeq 1.5\times10^{-19}\ \mathrm{s}$, so $v\Delta t$ cannot exceed atomic dimensions even for relativistic velocities. Hence this is a excellent approximation.

In particular, our goal is to determine how σ changes with time. One possibility is that σ slides along with *q*, moving parallel to the surface. However, we can discard this model immediately because σ is a layer of thickness zero, so this leads to an infinite current density. Thus the screening charge can be expected to rise out of the conductor as *q* approaches then fade back into the conductor after *q* passes. Our task now is to describe this action quantitatively.

The key point is that the finite response time of the system can be expected to result in a delay in updating σ. Therefore, from the perspective of both the conductor and *q*, the image charge $(-q)$ exists but is slightly retarded location relative to its electrostatics position. Hence from the conductor perspective cancellation is no longer exact. Therefore, a field will exist, and a current will flow. To determine the current, let the position of *q* be $\vec{R}_o = \vec{r}_o + \vec{v}_o t$ and let the time delay be Δt. Then the potential at any point $\vec{r}$ in the conductor is

$$\Delta\phi = \frac{q}{|\vec{r} - \vec{r}_o - \vec{v}_o t|} + \frac{(-q)}{|\vec{r} - \vec{r}_o - \vec{v}_o (t - \Delta t)|} \tag{5.12a}$$

$$= \frac{q}{R} - \frac{q}{|\vec{R} + \vec{v}_o \Delta t|} \tag{5.12b}$$

$$\simeq \frac{q}{R} - \frac{q}{R}\left(1 + \frac{\vec{v}_o \Delta t}{\vec{R}}\right)^{-1/2} \tag{5.12c}$$

$$\simeq \frac{(q\vec{v}_o \Delta t)\cdot \vec{R}}{R^3} \tag{5.12d}$$

where $\vec{R} = \vec{r} - \vec{r}_o - \vec{v}_o t$. Note that Eq. (5.12d) describes the potential in the coordinate system where *q* is at rest. As we shall see in Ch. 7, Eq. (5.12d) is the potential of a dipole $\vec{p} = q\vec{v}\Delta t$, where $\vec{v}\Delta t$ is the distance between *q* and its image $(-q)$ as viewed from the conductor. Evaluating $\vec{E} = -\nabla\phi$, we find the current in the conductor to be

$$\vec{J} = \sigma_c \vec{E} = \sigma_c \frac{3\vec{R}(\vec{R}\cdot\vec{p}) - R^2\vec{p}}{R^5} \tag{5.13}$$

The result is general, pertaining to any direction of $\vec{v}$.

Equation (5.13) exhibits the expected characteristics, which can be appreciated more easily by evaluating it at various locations $\vec{r}$ in the conductor when *q* passes over the origin, i.e., when its location is $\vec{r}_o + \vec{v}_o t = \hat{z}d$. To be specific, let *q* move in the positive *x* direction with a velocity $\vec{v}_o = \hat{x}v$, and evaluate $\vec{J}$ just under the surface, where $\vec{r} = x\hat{x}$. Then

$$\vec{R} = \hat{x}x - \hat{z}d . \tag{5.14}$$

With $\vec{p} = \hat{x}(qv\Delta t)$, Eq. (5.13) reduces to

$$\vec{J}(\hat{x}x) = \frac{(2x^2 - d^2)\hat{x} - 3\hat{z}xd}{(d^2 + x^2)^{5/2}}(\sigma_c qv\Delta t) . \tag{5.15}$$

For the observer directly below *q*, we have $\vec{R} = -\hat{z}(z + d)$, in which case

$$\vec{J}(-\hat{z}z) = -\frac{\sigma_c qv\Delta t}{(d + z)^{3/2}}\hat{x} . \tag{5.16}$$

Thus the system behaves as expected, positive charge flows away from the surface ahead of *q*, toward the surface behind *q*, and in the direction opposite $\vec{v}$ directly below.

It is also useful to consider the force on *q* using Coulomb's Law. From the perspective of *q*, the image charge is located at

$$\vec{r} = -\hat{z}d - \hat{x}v\Delta t , \tag{5.17}$$

in which case

$$\vec{F}_{12} = -\frac{q^2(\hat{z}d - (-\hat{z}d - \hat{x}v\Delta t))}{|-\hat{x}\Delta t - 2d|^3} \tag{5.18a}$$

$$\simeq \frac{q^2}{8d^2}\left(-2\hat{z} - \hat{x}v\Delta t\right) \tag{5.18b}$$

In addition to the attractive force pulling *q* toward the conductor, we see that the induced charge also exerts a drag, causing a power dissipation of

$$P = \vec{F}\cdot\vec{v} = -\frac{q^2v^2\Delta t}{8d^2} . \tag{5.19}$$

The configuration is therefore understood.

D. Examples where $\phi(\vec{r})$ is given on a plane.

In this and the next section we evaluate Eq. (5.3) for various configurations, following the advice in Sec. A to avoid series solutions whenever possible. This section considers examples where the potential is given on the $z = 0$ plane, so the Dirichlet Green function is the relevant kernel. As a starting example, suppose the lower half of the $z = 0$ plane is at a potential $\phi(x, y, 0) = V_o$ and the top half is at $\phi = 0$. Then

$\phi(x, y, 0) = V_o$ for $y \le 0$;

$$= 0 \text{ for } y > 0. \tag{5.20}$$

Then by Green's Theorem, Eq. (5.3),

$$\begin{aligned}
\phi(\vec{r}) &= \frac{zV_o}{2\pi}\int_{-\infty}^{\infty} dx' \int_{-\infty}^{0} dy' \frac{1}{\left((x-x')^2+(y-y')^2+z^2\right)^{3/2}} \\
&= \frac{zV_o}{2\pi}\int_{-\infty}^{0} \frac{2dy'}{(y-y')^2+z^2} \\
&= \frac{zV_o}{\pi}\left(\frac{1}{z}\tan^{-1}\frac{y'-y}{z}\right)_{-\infty}^{z} \\
&= V_o\left(\frac{1}{2}-\frac{1}{\pi}\tan^{-1}\frac{y}{z}\right).
\end{aligned} \tag{5.21}$$

We see by inspection that Eq. (5.21) reduces as it should: as $z \to 0$, $\phi = V_o$ for $y \le 0$ and $\phi = 0$ above.

As a second example, let V_o cover only the strip $-a \le y \le a$, and be zero elsewhere. Repeating the above calculation gives

$$\begin{aligned}
\phi(x,y) &= \frac{Vz}{2\pi}\int_{-a}^{a} dy' \frac{2}{(y-y')^2+z^2} \\
&= \frac{Vz}{\pi}\frac{1}{z}\tan^{-1}\frac{y'}{z}\Big|_{-a-y}^{a-y} \\
&= \frac{V}{\pi}\left(\tan^{-1}\frac{a+y}{z}+\tan^{-1}\frac{a-y}{z}\right)
\end{aligned} \tag{5.22}$$

which is consistent with Eq. (5.21).

E. Interpretation of G_N and G_D: the disc.

The Green functions $G_N(\vec{r},\vec{r}')$ and $G_D(\vec{r},\vec{r}')$ are defined by different boundary conditions, leading to solutions that are qualitatively different even for configurations that are dimensionally identical. These differences are the topic of this section. We investigate them by considering a disc of radius *a* centered on the *z* axis and lying in the $z = 0$ plane, first with a uniform charge density σ suspended in empty space, then with a specified uniform normal field, and finally with a specified uniform potential. These three examples involve the free-space, Neumann, and Dirichlet Green functions, respectively. By comparing results, we achieve a better understanding of GF solutions of boundary-condition problems in general. The intellectual challenge of dealing with a disc and a conducting surface both at $z = 0$ in the GF examples is resolved by considering the disc to be located at an infinitesimal distance δz in front of the $z = 0$ plane.

(a) We consider first a disc of constant charge density σ embedded in otherwise empty space, not only for its simplicity but also because it introduces the mathematics necessary to deal with the other GF configurations. Then in this case $G(\vec{r},\vec{r}\,') = 1/|\vec{r}-\vec{r}\,'|$ and the relevant part of Eq. (5.3) is the volume integral. Therefore

$$\phi(\vec{r}) = \int_V d^3r'\ \rho(\vec{r}\,')G(\vec{r},\vec{r}\,') = \int_0^a \rho'\,d\rho' \int_0^{2\pi} d\varphi' \frac{\sigma}{|\vec{r}-\vec{r}\,'|} \tag{5.23a,b}$$

$$= \int_0^a \rho'\,d\rho' \int_0^{2\pi} d\varphi' \frac{\sigma}{\sqrt{(x-\rho'\cos\varphi')^2 + (y-\rho'\sin\varphi')^2 + z^2}}, \tag{5.23c}$$

where the cylindrical coordinate ρ' is not to be confused with the charge density ρ. This is an elliptic integral. However, it reduces to elementary functions if the observer is on the *z* axis. In this case we find

$$\phi(0,0,z) = \int_0^a \rho'\,d\rho' \int_0^{2\pi} d\varphi' \frac{\sigma}{\sqrt{x'^2+y'^2+z^2}} = \int_0^a \rho'\,d\rho' \int_0^{2\pi} d\varphi' \frac{\sigma}{\sqrt{\rho'^2+z^2}} \tag{5.24a}$$

$$= 2\pi\sigma\sqrt{\rho'^2+z^2}\Big|_0^a \tag{5.24b}$$

$$= 2\pi\sigma\left(\sqrt{a^2+z^2} - |z|\right). \tag{5.24c}$$

The absolute-value signs follow because $\sqrt{z^2} = |z|$. This is critical for ensuring that $\vec{E}$ points away from the disc on both sides, as is easily verified. The solution is symmetric, as expected for the configuration. Applying Gauss' Theorem and integrating over a Gaussian pillbox straddling the interface yields a surface charge density of σ, as expected.

For $|\vec{r}| >> a$

$$\phi(\vec{r}) = \int_0^a \rho'\,d\rho' \int_0^{2\pi} d\varphi' \frac{\sigma}{|\vec{r}-\vec{r}\,'|} \cong \int_0^a \rho'\,d\rho' \int_0^{2\pi} d\varphi' \int_{-\infty}^{\infty} dz' \frac{\sigma\delta(z')}{\sqrt{r^2 - 2\vec{r}\cdot\vec{r}\,'}}$$

$$\cong \frac{\sigma}{r}\int_0^a \rho'\,d\rho' \int_0^{2\pi} d\varphi' \left(1 + x\rho'\cos\varphi' + y\rho'\sin\varphi'\right)$$

$$= \frac{\pi a^2\sigma}{r}. \tag{5.25}$$

This is again what we expect. For a remote observer the disc appears as a point charge $q = \pi a^2\sigma$ located at the origin. Finer details cannot be resolved. In a multipole expansion, this is the zero-order, or monopole, term. If the multipole calculation is carried to higher orders, only the even-order terms (quadrupole, …) contribute, as expected by symmetry. Multipole expansions are best suited to spherical coordinates, so are discussed in Ch. 7.

(b) We now consider the configuration where V is the half-plane $z \geq 0$ and the normal field is specified. Let $\vec{E}_n = E_n \delta(z)\hat{z}$ for $\rho \leq a$, and zero elsewhere. This is a Neumann problem. With $\rho = 0$ in the VOI, $\phi(\vec{r})$ is given by

$$\phi(\vec{r}) = \frac{1}{4\pi}\int_S d^2r' G_N(\vec{r},\vec{r}')\hat{n}\cdot\nabla_{\vec{r}'}\phi(\vec{r}'), \tag{5.26a}$$

where

$$G_N(\vec{r},\vec{r}') = \frac{1}{\sqrt{(x-x')^2+(y-y')^2+(z-z')^2}} + \frac{1}{\sqrt{(x-x')^2+(y-y')^2+(z+z')^2}}. \tag{5.26b}$$

This is to be evaluated at $z' = 0$, with $\hat{n} = -\hat{z}$ and $\hat{n}\cdot\nabla\phi = (-\hat{z})(-\hat{z}E_n) = E_n$ for $\rho \leq a$. At $z' = 0$ both terms in G_N are equal, therefore

$$\phi(\vec{r}) = \frac{E_n}{2\pi}\int_0^a \rho' d\rho' \int_0^{2\pi} d\varphi' \frac{1}{\left((x-\rho'\cos\varphi')^2+(y-\rho'\sin\varphi')^2+z^2\right)^{1/2}}. \tag{5.27}$$

The calculation proceeds as with the disc in empty space. Equation (5.30) is an elliptic integral, but with the observer on the *z* axis the result is

$$\phi(0,0,z) = \frac{E_n}{2\pi}2\pi\int_0^a \frac{1}{2}d(\rho'^2)\frac{1}{\sqrt{\rho'^2+z^2}} = \frac{E_n}{2}2\sqrt{\rho'^2+z^2}\Big|_0^a$$
$$= E_n\left(\sqrt{a^2+z^2}-z\right). \tag{5.28}$$

Noting that the boundary condition for the Neumann Green function is $\hat{n}\cdot\vec{E} = 0$ on the $z = 0$ plane, the application of Gauss' Theorem to $\nabla\cdot\vec{E} = 4\pi\rho$ now yields a surface charge density given by $E_n = 4\pi\sigma$, which is twice as large for a given σ than for the free-standing disc. This is also seen in the far-field limit, where the same calculation yields

$$\phi(\vec{r}) \cong \frac{E_n a^2}{2r} = 2\frac{\sigma\pi a^2}{r}, \tag{5.29}$$

We return to this point after investigating the Dirichlet solution.

(c) Now let $\phi(r) = V$ for $\rho \leq a$ on the $z = 0$ plane and be zero elsewhere: This is the Dirichlet version, where

$$G_D(\vec{r},\vec{r}') = \frac{1}{\sqrt{(x-x')^2+(y-y')^2+(z-z')^2}} - \frac{1}{\sqrt{(x-x')^2+(y-y')^2+(z+z')^2}}. \tag{5.30}$$

$\phi(\vec{r})$ is now given by the Dirichlet surface term. For $z \geq 0$,

$$\phi(\vec{r}) = -\frac{1}{4\pi}\int_S d^2r'\hat{n}\cdot\nabla_{\vec{r}}G(\vec{r},\vec{r}'). \tag{5.31}$$

Evaluating this at $z'=0$, with $\hat{n}=-\hat{z}$ and $\phi = V$ for $\rho' \leq 0$ gives

$$\phi(\vec{r}) = \frac{zV}{2\pi}\int_0^a \rho' d\rho' \int_0^{2\pi} d\varphi' \frac{1}{\left((x-\rho'\cos\varphi')^2+(y-\rho'\sin\varphi')^2+z^2\right)^{3/2}}. \tag{5.32}$$

On the *z* axis this becomes

$$\phi(0,0,z) = \frac{zV}{2\pi}2\pi\int_0^a \rho' d\rho' \frac{1}{(\rho'^2+z^2)^{3/2}} = \frac{1}{2}zV\left(-\frac{2}{\sqrt{\rho'^2+z^2}}\right)_0^a$$

$$= V\left(1-\frac{z}{\sqrt{a^2+z^2}}\right). \tag{5.33}$$

The result clearly reduces to V when $z=0$. In the far-field region we obtain

$$\phi(\vec{r}) = \frac{zV}{2\pi}\int_0^a \rho' d\rho' \int_0^{2\pi} d\varphi' \frac{1}{\left(|\vec{r}-\vec{r}'|\right)^{3/2}}\bigg|_{z'=0} \tag{5.34a}$$

$$\cong \frac{zVa^2}{r^3}. \tag{5.34b}$$

Recalling Sec. D, this is the potential of a dipole of strength Va^2 oriented in the positive *z* direction. Thus the first nonvanishing term in this case is the dipole. The observer sees no net charge at all.

We can now make some comments about the physics of Green functions, with reference to the disc in empty space. The Neumann Green function generates a charge on the conductor that ensures that the field between it and the disc is zero. Hence σ on the conductor is the same as that on the disc. When the observer is far enough away, both charges are viewed as a point, and since both are real charges, the observer sees the equivalent of $2q$. In a multipole expansion the even symmetry of the configuration means that all odd expansion terms (dipole, octupole, …) vanish.

In the Dirichlet case the Green function generates a σ on the conductor that ensures that the potential between it and the disc is zero. Hence σ on the conductor is again the same as that on the disc but of opposite sign. With the zero-order term in the expansion vanishing, the first nonzero contribution is the dipole. The odd symmetry of the configuration means that all even expansion terms (monopole, quadrupole,…) vanish.

F. Finite configurations in 3D: the cube.

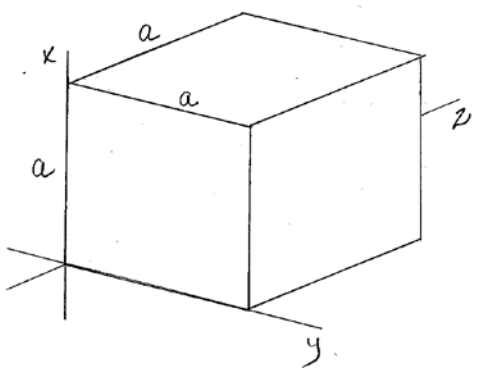

The simplest example of a rectilinear configuration is the cube of sides of length a, embedded in a coordinate system with one corner at the origin and *x*, *y*, and *z* axes parallel to the appropriate edges, as shown in the diagram. Following the recipe in Sec. B, we attempt an image-charge solution and quickly realize that this is hopeless, even for a charge *q* in a high-symmetry point such as the center. Locating six charges $(-q)$ at the image points of the six facets requires additional charges *q* to cancel potentials at back-surface facets and even though contributions die off as r^{-1}, the additions quickly get out of hand. This is analogous to the physics of Ewald sums in calculating the dielectric responses of highly ionic solids, where convergence is also agonizingly slow but can be speeded up somewhat by pairing charges to form dipoles, whose contributions drop off as r^{-3} (see previous section).

Again, following the recipe of Sec. B, the Laplacian is

$$\nabla^2 = \left(\frac{\partial^2}{\partial x^2} + \frac{\partial^2}{\partial y^2} + \frac{\partial^2}{\partial z^2} \right). \tag{5.35}$$

Using the *x* direction as an example, the negative-curvature eigenfunctions are $e^{\pm ikx}$ and their linear combinations $\sin kx$ and $\cos kx$. The positive-curvature eigenfunctions are $e^{\pm \kappa x}$ and their linear combinations $\sinh(\kappa x)$ and $\cosh(\kappa x)$. Since we want functions on the remaining facets to vanish, with the coordinate system shown we set $k = \pi l / a$ where *l* is an integer, with similar quantization for the sine functions in the *y* and *z* directions. The orthogonality relation for the sine functions is easily shown to be

$$\int_0^a dx \sin\left(\frac{\pi l}{a}\right) \sin\left(\frac{\pi l'}{a}\right) = \frac{a}{2} \delta_{ll'}. \tag{5.36}$$

These are the tools that we need to solve the configuration.

As the first case, assume that the potential is given as $\phi(x, y, 0) = V(x, y)$ on the $z = 0$ face, and the objective is to find it everywhere in the cube. Although this could be solved by Green functions, the simplest approach is a direct expansion of $\phi(\vec{r})$ where every term satisfies Laplace's Equation. This leads to the generic expansion term

$$\phi_{lm}(\vec{r}) = A_{lm} \sin(k_l x) \sin(k_m y) \sinh(k_{lm}(a - z)), \tag{5.37}$$

where A_{lm} is a constant. Because $\phi_{lm}(\vec{r})$ must be zero on all sides except $z = 0$ AND satisfy Laplace's Equation on a term-by-term basis, we conclude that

$$k_l = \pi l / a, \quad k_m = \pi m / a, \quad k_{lm} = \sqrt{k_l^2 + k_m^2}, \tag{5.38}$$

where *l* and *m* are integers. We choose this form for the sinh function so it vanishes on the $z = a$ face but is positive definite elsewhere. With these values for the k_j, each term satisfies the conditions stated above.

Our expansion of $\phi(\vec{r})$ is therefore

$$\phi(\vec{r}) = \sum_{l=1}^{\infty}\sum_{m=1}^{\infty} A_{lm} \sin(\frac{\pi l}{a}x)\sin(\frac{\pi m}{a}y)\sinh(k_{lm}(a-z)) . \tag{5.40}$$

The next step is to obtain the A_{lm}. To do this we set $z = 0$ in Eq. (5.40), multiply both sides by $\sin(\frac{\pi l'}{a}x)\sin(\frac{\pi m'}{a}y)$, then integrate *x* and *y* from 0 to *a*, taking advantage of Eq. (5.39). The result is

$$A_{lm} = \frac{4V_{lm}}{a^2 \sinh(k_{lm}a)} , \tag{5.41a}$$

where

$$V_{lm} = \int_0^a dx \int_0^a dy V(x,y)\sin(\frac{\pi l}{a}x)\sin(\frac{\pi m}{a}y) \tag{5.41b}$$

is the (l,m) Fourier transform of $V(x,y)$. Note that the terms converge exponentially for large *l* and *m*, a significant advantage for numerical evaluation. Also, all the information contained in $V(x,y)$ is contained in the set of coefficients $\{V_{lm}\}$. If the surface potential is nonzero on other faces, the procedure is repeated for each face with appropriate changes in the arguments of the functions.

The solution also contains physics. With $k_{lm} = \frac{\pi}{a}\sqrt{l^2 + m^2}$, we see that the contribution of the *lm* harmonic decays exponentially away from the $z = 0$ face with a decay length of $1/k_{lm}$. Thus the higher the harmonic, the higher the resolution, but also the higher the attenuation away from the surface. This is the tradeoff faced in near-field optical microscopy.

We next consider the third approach, expanding $G_D(\vec{r},\vec{r}')$ as a triple product (and triple summation) of orthogonal functions, where in Cartesian coordinates

$$\nabla^2 G(\vec{r},\vec{r}') = -4\pi\delta(x-x')\delta(y-y')\delta(z-z') . \tag{5.42}$$

A triple product of orthogonal functions is allowed here because Eq. (5.42) is inhomogeneous. Therefore, the individual terms need not satisfy Laplace's Equation. The relevant expansion is

$$G_D(\vec{r},\vec{r}') = \sum_{l,m,n=1}^{\infty} A_{lmn} \sin(\frac{\pi l}{a}x)\sin(\frac{\pi m}{a}y)\sin(\frac{\pi n}{a}z) , \tag{5.43}$$

where l, m, n are integers. Again, the requirement that $G_D(\vec{r},\vec{r}') = 0$ on all sides is accomplished by picking a convenient origin and quantizing $\vec{k}$ as $k_x = \pi l/a$, etc. Substituting Eq. (5.43) in Eq. (5.42) yields

$$\nabla^2_{\vec{r}} G_D(\vec{r},\vec{r}') = \sum_{l,m,n=1}^{\infty} \left(-\frac{\pi^2}{a^2}(l^2+m^2+n^2) \right) A_{lmn} \sin(\frac{\pi l}{a}x)\sin(\frac{\pi m}{a}y)\sin(\frac{\pi n}{a}z)$$

$$= -4\pi\delta(x-x')\delta(y-y')\delta(z-z'). \qquad (5.44)$$

We now multiply both sides of Eq. (5.44) by $\sin(\frac{\pi l'}{a})\sin(\frac{\pi m'}{a})\sin(\frac{\pi n'}{a})$ and integrate each coordinate from 0 to a. From Eq. (5.39) this converts Eq. (5.44) to

$$-\frac{a^3}{8}\frac{\pi^2}{a^2}\left(l'^2+m'^2+n'^2\right)A_{l'm'n'}$$

$$= -4\pi \int_0^a dx \int_0^a dy \int_0^a dz \sin\left(\frac{\pi l'}{a}x\right)\sin\left(\frac{\pi m'}{a}y\right)\sin\left(\frac{\pi n'}{a}z\right)\delta(x-x')\delta(y-y')\delta(z-z')$$

$$= -4\pi \sin\left(\frac{\pi l'}{a}x'\right)\sin\left(\frac{\pi m'}{a}y'\right)\sin\left(\frac{\pi n'}{a}z'\right). \qquad (5.45)$$

Finishing off the mathematics gives

$$A_{lmn} = \frac{32}{\pi a(l^2+m^2+n^2)}\sin\left(\frac{\pi l}{a}x'\right)\sin\left(\frac{\pi m}{a}y'\right)\sin\left(\frac{\pi n}{a}z'\right), \qquad (5.46)$$

so

$$G_D(\vec{r},\vec{r}') = \frac{32}{\pi a}\sum_{lmn=1}^{\infty}\left(\frac{1}{(l^2+m^2+n^2)}\sin\left(\frac{\pi l}{a}x\right)\sin\left(\frac{\pi l}{a}x'\right) \right.$$

$$\left. \times \sin\left(\frac{\pi m}{a}y\right)\sin\left(\frac{\pi m}{a}y'\right)\sin\left(\frac{\pi n}{a}z\right)\sin\left(\frac{\pi n}{a}z'\right)\right). \qquad (5.47)$$

Equation (5.47) is obviously symmetric in $\vec{r}$ and $\vec{r}'$, and vanishes for either $\vec{r}$ and $\vec{r}'$ on any of the cube faces. With the aid of the completeness relation

$$\sum_{l=1}^{\infty}\sin\left(\frac{\pi l}{a}x\right)\sin\left(\frac{\pi l}{a}x'\right) = \frac{a}{2}\delta(x-x'), \qquad (5.48)$$

we see that Eq. (5.2) is satisfied as well. In fact, given Eq. (5.48), we could have written Eq. (5.47) by inspection. The terms of Eq. (5.5.47) converge slowly as $1/(l^2+m^2+n^2)$. Thus while this series is relatively easy to derive, it is not practical for evaluation.

In the third approach, we write $G_D(\vec{r},\vec{r}')$ as a double summation where each term satisfies Laplace's Equation, analogous to what was done for the one-dimensional configuration in Ch. 3. Sinh functions are obviously needed to balance the negative

eigenvalues from the sine functions. But the solution requires a function that vanishes on opposite sides. Since the sinh function has only one zero, it appears that we must look elsewhere. However, by patching together two sinh functions so the result is continuous at the junction but has different first derivatives, as done in one dimension in Ch. 3, we can make it work.

Assuming again that $V(x, y)$ is specified on the $z = 0$ face, the orthogonal functions must be associated with the *x* and *y* directions and *z* treated as the special case. Accordingly, we consider the trial solution

$$G_D(\vec{r},\vec{r}\,') = \sum_{l,m=1}^{\infty} A_{lm} \sin(k_l x)\sin(k_m y)\sinh(k_{lm} z_<)\sinh(k_{lm}(a - z_>)), \tag{5.49}$$

where k_l, k_m, and k_{lm} are defined above. As usual, $z_<$ and $z_>$ are the lesser or greater, respectively, of z' and *z*. Each term therefore satisfies Laplace's Equation if $z \neq z'$. This is also consistent with Eq. (5.2), because $\delta(z - z')$ is zero except at $z = z'$. Equation (5.49) also satisfies the continuity condition because at $z = z'$ the product of the sinh functions has the value

$$\sinh(k_{lm} z)\sinh(k_{lm}(a - z') = \sinh(k_{lm} z')\sinh(k_{lm}(a - z)). \tag{5.50}$$

We now determine the A_{lm}. As usual, this is done by working with the defining equation

$$\nabla^2_{\vec{r}} G_D(\vec{r},\vec{r}\,') = -4\pi\delta(\vec{r} - \vec{r}\,') = -4\pi\delta(x - x')\delta(y - y')\delta(z - z'), \tag{5.51}$$

although the path to success here is different. Substituting Eq. (5.49) in Eq. (5.51) yields

$$\left(\frac{\partial^2}{\partial x^2} + \frac{\partial^2}{\partial y^2} + \frac{\partial^2}{\partial z^2}\right) G_D(\vec{r},\vec{r}\,') = -4\pi\delta(x - x')\delta(y - y')\delta(z - z')$$

$$= \sum_{lm=1}^{\infty}\left(-\frac{\pi^2}{a^2}(l^2 + m^2) + \frac{\partial^2}{\partial z^2}\right) A_{lm} \sin\left(\frac{\pi l}{a} x\right)\sin\left(\frac{\pi m}{a} y\right)$$

$$\times \sinh(\kappa_{lm} z_<)\sinh(\kappa_{lm}(a - z_>)). \tag{5.52}$$

At this point we cannot evaluate the operator $\partial^2/\partial z^2$, because we do not know whether *z* is greater or less than z'. Accordingly, we do not know which of the two sinh functions to differentiate.

We proceed by first capitalizing on orthogonality. Multiplying both sides by $\sin\left(\frac{\pi l'}{a} x\right)\sin\left(\frac{\pi m'}{a} y\right)$ and integrating *x* and *y* from 0 to *a* gives

$$-4\pi \sin\left(\frac{\pi l'}{a} x'\right)\sin\left(\frac{\pi m'}{a} y'\right)\delta(z - z')$$

$$= \frac{a^2}{4} A_{l'm'} \left(-k_{l'm'}^2 + \frac{\partial^2}{\partial z^2} \right) \sinh(k_{l'm'} z_<) \sinh(k_{l'm'}(a - z_>)) . \qquad (5.53)$$

Next, again following what we did in one dimension, integrate Eq. (5.53) over a vanishingly small range from $z = z' - \delta z$ to $z = z' + \delta z$. This eliminates the delta function and converts $\partial^2 / \partial z^2$ to $\partial / \partial z$. In the limit $\delta \to 0$ the contribution of $(-k_{l'm'}^2)$ to the integral vanishes, and we are left with

$$-4\pi \sin\left(\frac{\pi l'}{a} x'\right) \sin\left(\frac{\pi m'}{a} y'\right)$$

$$= \frac{a^2}{4} A_{l'm'} \frac{\partial}{\partial z} \sinh(k_{l'm'} z_<) \sinh(k_{l'm'}(a - z_>)) \Big|_{z'-\varepsilon}^{z'+\varepsilon} . \qquad (5.54)$$

Being located away from the singularity the limits on the right side are well defined. For $z < z'$ we have

$$\frac{\partial}{\partial z} G_D(\vec{r}, \vec{r}') \Big|_{z<z'} = \sum_{lm=1}^{\infty} A_{lm} k_{lm} \sin\left(\frac{\pi l}{a} x\right) \sin\left(\frac{\pi m}{a} y\right)$$

$$\times \cosh(k_{lm} z) \sinh(k_{lm}(a - z')) , \qquad (5.455a)$$

while for $z > z'$ we have

$$\frac{\partial}{\partial z} G_D(\vec{r}, \vec{r}') \Big|_{z>z'} = -\sum_{lm=1}^{\infty} A_{lm} \kappa_{lm} \sin\left(\frac{\pi l}{a} x\right) \sin\left(\frac{\pi m}{a} y\right)$$

$$\times \sinh(\kappa_{lm} z') \cosh(\kappa_{lm}(a - z)) . \qquad (5.55b)$$

Taking the difference gives

$$-4\pi \sin\left(\frac{\pi l'}{a} x'\right) \sin\left(\frac{\pi m'}{a} y'\right)$$

$$= \frac{a^2}{4} A_{l'm'} k_{l'm'} \left(-\sinh(k_{l'm'} z') \cosh(k_{l'm'}(a - z')) - \cosh(k_{l'm'} z') \sinh(k_{l'm'}(a - z')) \right)$$

$$= -\frac{a^2}{4} A_{l'm'} k_{l'm'} \sinh(k_{l'm'} a) . \qquad (5.56)$$

Therefore

$$A_{lm} = \frac{16\pi \sin\left(\frac{\pi l}{a} x'\right) \sin\left(\frac{\pi m}{a} y'\right)}{a^2 k_{lm} \sinh(k_{lm} a)} \qquad (5.57)$$

and the coefficients are determined. The Green function is

$G_D(\vec{r}, \vec{r}') =$

$$\frac{16\pi}{a^2}\sum_{lm=1}^{\infty}\frac{\sin\left(\frac{\pi l}{a}x\right)\sin\left(\frac{\pi l}{a}x'\right)\sin\left(\frac{\pi l}{a}y\right)\sin\left(\frac{\pi l}{a}y'\right)\sinh(k_{lm}z_<)\sinh(k_{lm}(a-z_>))}{k_{lm}\sinh(k_{lm}a)}. \quad (5.58)$$

Note that the series converges exponentially for large *l* and *m*, leading to efficient evaluation. Therefore, from a computational perspective, the extra effort is well worth it.

We can close the loop between the previous triple-sum and the above double-sum solutions via the identity

$$\frac{\sinh(k_{lm}z_<)\sinh(k_{lm}(a-z_>))}{k_{lm}\sinh(k_{lm}a)}=\frac{2}{a}\sum_{n=1}^{\infty}\frac{\sin\left(\frac{\pi n}{a}z\right)\sin\left(\frac{\pi n}{a}z'\right)}{k_{lm}^2+\left(n\pi/a\right)^2}. \quad (5.59)$$

Just don't ask me to prove it.

G. Infinite configurations: Fourier representation of $1/|\vec{r}-\vec{r}'|$.

If the volume of interest extends to infinity on one or more directions, then the approach described in Sec. E must be modified. In the infinite directions discrete summations become integrations, terms become integrands, and continuum concepts apply.

Consider first the cube where $\phi(x,y,0)=V(x,y)$ is given on the surface $z=0$ and the surface $z=a$ recedes to infinity. Equation (5.26a) clearly won't work, but if we replace the sinh function with the decreasing exponential:

$$\phi(\vec{r})=\sum_{l=1}^{\infty}\sum_{m=1}^{\infty}A_{lm}\sin(\frac{\pi l}{a}x)\sin(\frac{\pi m}{a}y)e^{-k_{lm}z}, \quad (5.60)$$

then everything goes through as before except for an obvious minor modification of the expansion coefficients. The potential decays exponentially in the *z* direction. A penetration depth

$$\lambda_{lm}=\frac{1}{k_{lm}}=\frac{a}{\pi\sqrt{l^2+m^2}} \quad (5.61)$$

is associated with each term. It is seen that the higher the harmonic, the shorter the penetration depth. The result is relevant for near-field optical microscopy, where higher resolution (larger values of k_{lm}) leads to greater attenuation. The competition between resolution and attenuation is an inevitable consequence of physical phenomena that depend on the Laplacian operator. Near-field optical microscopy was recognized in 2014 by the Nobel Prize in Chemistry.

Consider next the situation where all boundaries recede to infinity except the plane $z=0$, with $\phi(\vec{r})$ specified on this plane and the volume of interest covering the half-space $z\geq 0$. The discrete oscillatory eigenfunctions of the Cartesian Laplacian in the confined situation become plane waves $e^{i\vec{k}\cdot\vec{r}}$ in the continuum. The orthogonality condition for plane waves is

$$\int_{-\infty}^{\infty} d^3r\, e^{i(\vec{k}-\vec{k}')\cdot\vec{r}} = (2\pi)^3 \delta(\vec{k}-\vec{k}')\,. \tag{5.62a}$$

The reciprocal-space equivalent is

$$\int_{-\infty}^{\infty} d^3k\, e^{i\vec{k}\cdot(\vec{r}-\vec{r}')} = (2\pi)^3 \delta(\vec{r}-\vec{r}')\,. \tag{5.62b}$$

The integrand that satisfies Laplace's Equation is obviously

$$\phi(\vec{r}) = \int_{-\infty}^{\infty} dk_x \int_{-\infty}^{\infty} dk_y A(k_x, k_y) e^{ik_x x} e^{ik_y y} e^{-k_{xy} z}\,, \tag{5.63a}$$

where

$$k_{xy} = \sqrt{k_x^2 + k_y^2}\,. \tag{5.63b}$$

Given that $\phi(x, y, 0) = V_o(x, y)$, the coefficient $A(k_x, k_y)$ is given by

$$A(k_x, k_y) = \frac{1}{(2\pi)^2} \int_{-\infty}^{\infty} dx \int_{-\infty}^{\infty} dy V(x, y) e^{-ik_x x} e^{-ik_y y}\,, \tag{5.64}$$

and the formal solution is obtained. If the volume of interest is terminated at the plane $z = a$, also held at zero potential, then the decreasing exponential in Eq. (5.63a) would be replaced by $\sinh\left(k_{lm}(a-z)\right)$, thereby modifying Eq. (5.64). Details are left as an exercise.

The use of these equations is illustrated with further examples. Consider the situation where the volume of interest is the half-space $z \geq 0$. Let $V(x, y) = V$ for $|\, y \,| \leq a$ and zero elsewhere. This is the same configuration that was discussed in Sec. D, which was solved there using the Dirichlet Green function. The integration over *x* yields $2\pi\delta(k_x)$, which eliminates the integration over k_x, one of the factors of 2π, and establishes $k_{xy} = |\, k_y \,|$. Working through the *y* integration and dropping the subscript *y* of k_y, we find

$$\int_{-a}^{a} dy V e^{-iky} = V \frac{e^{-iky}}{-ik}\bigg|_{-a}^{a} = \frac{2V\sin(ka)}{k}\,. \tag{5.65}$$

Thus

$$A(k) = \frac{V\sin(ka)}{\pi k}\,. \tag{5.66}$$

It follows that

$$\phi(y, z) = \frac{V}{\pi} \int_{-\infty}^{\infty} dk \frac{\sin(ka)}{k} e^{iky} e^{-|k|z}\,. \tag{5.67}$$

Equation (5.67) can be simplified by noting that $\sin(ka)/k$ is even in *k*, as is $e^{-|k|z}$. Since the range of the integral is also even, we can discard the odd part $i\sin(ky)$ of e^{iky} and write the integral as

$$\phi(y,z) = \frac{2V}{\pi}\int_0^\infty dk\,\frac{\sin(ka)}{k}\cos(ky)e^{-kz}\,, \tag{5.68}$$

where we have changed the range of the integral to conform to standard integral tables. However, it is necessary to proceed with caution. One that I consulted listed this as the unintuitive expression

$$\phi(y,z) = \frac{2V}{\pi}\left(\frac{1}{2}\tan^{-1}\frac{2za}{z^2-a^2+y^2}\right)+\frac{\pi}{2}u(a^2-y^2-z^2)\,. \tag{5.69}$$

A more productive approach is to take advantage of the trigonometric expansion

$$\sin(ka)\cos(ky) = \frac{1}{2}\big(\sin k(a+y)+\sin k(a-y)\big). \tag{5.70}$$

This yields the much more understandable result

$$\phi(y,z) = \frac{V}{\pi}\left(\tan^{-1}\frac{a+y}{z}+\tan^{-1}\frac{a-y}{z}\right). \tag{5.71}$$

This expression vanishes for large *z*, and is seen by inspection to satisfy the boundary conditions in the limit $z\to 0$.

We consider next the Fourier representation of the Green function of empty space. Let

$$G(\vec{r}) = \int_{-\infty}^{\infty} d^3k\,A(\vec{k})\,e^{i\vec{k}\cdot\vec{r}}\,, \tag{5.72}$$

and substitute Eq. (5.72) in the defining equation

$$\nabla^2 G(\vec{r},\vec{r}') = -\int_{-\infty}^{\infty} k^2 d^3k\,A(\vec{k})\,e^{i\vec{k}\cdot(\vec{r}-\vec{r}')} = -4\pi\delta(\vec{r}-\vec{r}')\,. \tag{5.73}$$

Taking advantage of orthogonality,

$$\int_{-\infty}^{\infty} d^3r\,e^{-i\vec{k}'\cdot\vec{r}}\left(-\int_{-\infty}^{\infty} k^2 d^3k\,A(\vec{k})\,e^{i\vec{k}\cdot(\vec{r}-\vec{r}')}\right)$$

$$= -(2\pi)^3\int_{-\infty}^{\infty} k^2 d^3k\,A(\vec{k})\,\delta(\vec{k}-\vec{k}') = -(2\pi)^3 k'^2\,A(\vec{k}')$$

$$= \int_{-\infty}^{\infty} d^3r\,e^{-i\vec{k}'\cdot\vec{r}}\big(-4\pi\delta(\vec{r}-\vec{r}')\big) = -4\pi\,e^{-i\vec{k}'\cdot\vec{r}}\,. \tag{5.74}$$

Thus

$$A(\vec{k}) = \frac{1}{2\pi^2}\frac{e^{-i\vec{k}\cdot\vec{r}'}}{k^2}. \tag{5.75}$$

In Cartesian coordinates

$$G(\vec{r},\vec{r}') = \frac{1}{2\pi^2}\int_{-\infty}^{\infty}\frac{d^3k}{k_x^2+k_y^2+k_z^2}e^{i\vec{k}\cdot(\vec{r}-\vec{r}')}. \tag{5.76}$$

Given the orthogonality condition Eq. (5.62b), this could have written down by inspection, proving that math doesn't have to be tedious.

Reversing the process, we evaluate $G(\vec{r},\vec{r}')$ from Eq. (5.76). Converting to spherical coordinates,

$$\begin{aligned} G(\vec{r},\vec{r}') &= \frac{1}{2\pi^2}\int_0^{\infty}k^2dk\int_{-1}^{1}d(\cos\theta)\int_0^{2\pi}d\varphi\frac{1}{k^2}e^{ik|\vec{r}-\vec{r}'|\cos\theta} \\ &= \frac{2\pi}{2\pi^2}\int_0^{\infty}dk\,\frac{e^{ik|\vec{r}-\vec{r}'|}-e^{-ik|\vec{r}-\vec{r}'|}}{ik\,|\vec{r}-\vec{r}'|} = \frac{2}{\pi\,|\vec{r}-\vec{r}'|}\int_0^{\infty}d(k\,|\vec{r}-\vec{r}'|)\frac{\sin(k\,|\vec{r}-\vec{r}'|)}{k\,|\vec{r}-\vec{r}'|} \\ &= \frac{1}{|\vec{r}-\vec{r}'|}. \end{aligned} \tag{5.77}$$

Although we already knew the answer, it's nice to see it work out systematically. Fourier representations for Dirichlet and Neuman Green functions follow by adding appropriate plane-wave terms to the integrand of Eq. (5.76).

In the above $A(\vec{k})$ is obtained indirectly. If we calculate the Fourier transform directly, we find a nonconvergent integral. This integral can be evaluated as a limit, and we consider that next. To calculate $A(\vec{k})$ directly, evaluate

$$\begin{aligned} A(\vec{k}) &= \frac{1}{(2\pi)^3}\int_{-\infty}^{\infty}d^3r\frac{e^{i\vec{k}\cdot\vec{r}}}{|\vec{r}-\vec{r}'|} \\ &= \frac{1}{(2\pi)^3}\int_{-\infty}^{\infty}d^3r\frac{e^{i\vec{k}\cdot(\vec{r}-\vec{r}')}e^{i\vec{k}\cdot\vec{r}'}}{|\vec{r}-\vec{r}'|} = \frac{e^{i\vec{k}\cdot\vec{r}'}}{(2\pi)^3}\int_{-\infty}^{\infty}d^3r\frac{e^{i\vec{k}\cdot(\vec{r}-\vec{r}')}}{|\vec{r}-\vec{r}'|} \\ &= \frac{e^{i\vec{k}\cdot\vec{r}'}}{(2\pi)^3}\int_0^{\infty}r^2dr\int_{-1}^{1}d(\cos\theta)\int_0^{2\pi}d\varphi\frac{e^{ikr\cos\theta}}{r} = \frac{2\pi\,e^{i\vec{k}\cdot\vec{r}'}}{(2\pi)^3}\int_0^{\infty}rdr\frac{e^{ikr\cos\theta}}{ikr}\bigg|_{\cos\theta=-1}^{1} \\ &= \frac{e^{i\vec{k}\cdot\vec{r}'}}{4\pi^2}\int_0^{\infty}dr\frac{2\sin kr}{k}\bigg| = \frac{e^{i\vec{k}\cdot\vec{r}'}}{2\pi^2k^2}\int_0^{\infty}d(kr)\sin(kr) \\ &= -\frac{e^{i\vec{k}\cdot\vec{r}'}}{2\pi^2k^2}\cos kr\Big|_0^{\infty}. \end{aligned} \tag{5.78}$$

The upper limit cannot be evaluated; it ranges between -1 and 1. We can fix this ambiguity by taking an average or assuming that the integral includes an implicit

convergent factor $e^{-\eta x}$. Both eliminates the contribution from the upper limit. After the calculation is completed, we take the limit $\eta \to 0$. The result is

$$A(\vec{k}) = \frac{e^{i\vec{k}\cdot\vec{r}}}{2\pi^2 k^2}, \tag{5.79}$$

which is Eq. (5.75). The assumed-convergence approach is often used to eliminate terms that cannot be evaluated by other means.

We can close a fairly large loop using Eq. (5.77) to describe the potential of a point charge *q* in empty space:

$$\phi(\vec{r}) = \frac{q}{|\vec{r} - \vec{r}_q|} = \frac{q}{2\pi^2} \int_{-\infty}^{\infty} d^3k \frac{1}{k^2} e^{i\vec{k}\cdot(\vec{r}-\vec{r}_q)}. \tag{5.80}$$

The inverse square dependence of the integrand on *k* in Eq. (5.80) is well known from quantum mechanics, and is a consequence of the long range of the Coulomb potential. Equation (5.80) was originally derived from Coulomb's Law for the force between point charges. Math is nothing if not consistent

The alternative empty-space representation of $G_D(\vec{r}, \vec{r}')$ analogous to that of Eq. (5.58) for the cube is also possible. Here, the k integration extends in only two dictions. The δ function in the third direction is generated by a discontinuity in the slope of a continuous function. This procedure will also be used to derive the Green function in spherical coordinates (see Jackson Sec. 3.9). Taking *z* as the special direction, the trial solution is

$$G(\vec{r}, z') = \int_{-\infty}^{\infty} dk_x dk_y A(k_x, k_y) e^{ik_x x} e^{ik_y y} e^{-k_{xy}|z-z'|}, \tag{5.81}$$

where

$$k_{xy} = \sqrt{k_x^2 + k_x^2}. \tag{5.82}$$

$|z - z'|$ is clearly continuous at $z = z'$, and its derivative in the *z* direction depends on whether *z* is larger or smaller than z'. To place this in the previous context, write

$$|z - z'| = z_> - z_<. \tag{5.83}$$

To determine the coefficients, substitute Eq. (5.65) in the defining equation and use orthogonality. The intermediate result is

$$\begin{aligned} \nabla_{\vec{r}}^2 G(\vec{r}, z') &= \int_{-\infty}^{\infty} dk_x \int_{-\infty}^{\infty} dk_y A(k_x, k_y) \left(-k_x^2 - k_y^2 + \frac{\partial^2}{\partial z^2} \right) e^{ik_x x} e^{ik_y y} e^{-k_{xy} a|z-z'|} \\ &= -4\pi\delta(x - x')\delta(y - y')\delta(z - z') \end{aligned} \tag{5.84}$$

Next, Fourier-transform the above by multiplying both sides by $e^{-i(k_x x + k_y y)}$, then integrate *x* and *y* from $-\infty$ to ∞. The result is

$$(2\pi)^2 A(k_x' k_y')\left(-k_x'^2 - k_y'^2 + \frac{\partial^2}{\partial z^2}\right)e^{-k_{xy}|z-z'|} = -4\pi e^{-ik_x' x'} e^{-ik_y' y'} \delta(z-z'). \tag{5.85}$$

We eliminate the δ function by integrating both sides of Eq. (5.85) over an infinitesimal range centered on z' then let $\delta \to 0$. This yields

$$(2\pi)^2 A(k_x' k_y') \int_{z'-\delta}^{z'+\delta} dz \left(-k_x'^2 - k_y'^2 + \frac{\partial^2}{\partial z^2}\right)e^{-k_{xy}|z-z'|} = -4\pi e^{-ik_x' x'} e^{-ik_y' y'}, \tag{5.86}$$

so

$$(2\pi)^2 A(k_x' k_y') \frac{\partial}{\partial z} e^{-k_{xy}'(z_> - z_<)}\Big|_{z'-\varepsilon}^{z'+\varepsilon} = (2\pi)^2 A(k_x' k_y')(-2k_{xy}')$$

$$= -4\pi e^{-ik_x' x'} e^{-ik_y' y'}. \tag{5.87}$$

Therefore

$$A(k_x, k_y) = \frac{1}{2\pi k_{xy}} e^{-ik_x x'} e^{-ik_y y,}, \tag{5.88}$$

and

$$G(\vec{r}, \vec{r}') = \frac{1}{2\pi} \int_{-\infty}^{\infty} \frac{dk_x dk_y}{k_{xy}} e^{ik_x (x-x')} e^{ik_y (y-y')} e^{-k_{xy}|z-z'|} \tag{5.89}$$

where k_{xy} is given by Eq. (5.82). As with the cube, reducing the number of integrations by one accelerates convergence, a factor of prime importance when these functions are evaluated numerically.

H. Two-dimensional configurations: Green's Theorem in 2D.

Two-dimensional solutions of the Laplace Equation are the foundation of the treatment of waveguides. Anticipating Ch. 13, we reduce the concepts developed in Sec. C to two dimensions. The concept of the cross section of a guide, given a propagation direction *z*, needs no explanation, but given the long range of the Coulomb potential the equivalent picture in electrostatics is less intuitive. We interpret 2D as describing the cross section of a cylindrical object, where we are far enough from the ends so that edge effects can be ignored. In the present context "cylindrical" means no *z* dependence, so the sidewalls are everywhere parallel to the *z* axis so the cross section is independent of *z*. The 2D equivalent of the point charge in 3D is a line of charge of uniform linear charge density Λ, just as the 1D equivalent is a sheet of uniform surface charge density σ. More on this below.

Consider first the situation where the potential $\phi(0, y) = V(y)$ is given on the side $x = 0$ of a square, with all other sides at zero potential. With no *z* dependence, Laplace's Equation reduces to

$$\left(\frac{\partial^2}{\partial x^2}+\frac{\partial^2}{\partial y^2}\right)\phi(x,y)=0\,. \tag{5.90}$$

The trial expansion is clearly

$$\phi(x,y)=\sum_{l=1}^{\infty}A_l\sin\left(\frac{\pi l}{a}y\right)\sinh\left(\frac{\pi l}{a}(a-x)\right). \tag{5.91}$$

Using orthogonality, the coefficients are

$$A_l=\frac{2}{a\sinh\pi l}\int_0^a dyV(y)\sin\frac{\pi l}{a}y\,, \tag{5.92}$$

and the problem is solved. In the process, what would have been a surface integral in 3D has become a *line* integral across the active edge.

If a (surface) charge density is present in the square, then it is necessary to use Green functions. The defining equation in two dimensions is

$$\nabla_t^2 G_t(x,x',y,y')=-4\pi\delta(x-x')\delta(y-y')\,. \tag{5.93}$$

In contrast to the 3D case, the 2D Green function is dimensionless. The subscript *t* denotes that the Laplacian and Green function are expressed in "transverse" coordinates only, which is terminology adapted from waveguides. The Green function of the first type follows from

$$G_t(\vec{r},\vec{r}')=\sum_{l,m}A_{lm}\sin\frac{\pi l}{a}x\,\sin\frac{\pi m}{a}y\,. \tag{5.94}$$

Substituting Eq. (5.77) in Eq. (5.76) and using orthogonality yields

$$A_{lm}=\frac{16}{\pi(l^2+m^2)}\sin\frac{\pi l}{a}x'\sin\frac{\pi m}{a}y'\,, \tag{5.95}$$

so

$$G_t(\vec{r},\vec{r}')=\sum_{l,m}\frac{16}{\pi(l^2+m^2)}\sin\frac{\pi l}{a}x\sin\frac{\pi l}{a}x'\sin\frac{\pi m}{a}y\,\sin\frac{\pi m}{a}y'\,. \tag{5.96}$$

The second type of Green function has the form

$$G_t(\vec{r},\vec{r}')=\sum_{l}A_l\sin\frac{\pi l}{a}y\,\sinh\frac{\pi l}{a}x_<\sinh\frac{\pi l}{a}(a-x_>)\,. \tag{5.97}$$

Substituting Eq. (5.96) in Eq. (5.93), using orthogonality, and integrating over the singularity gives

$$A_l=\frac{8}{l\sinh l\pi}\,\sin\frac{\pi l}{a}y'\,, \tag{5.98}$$

so

$$G_t(\vec{r},\vec{r}') = \sum_l \frac{8}{l \sinh l\pi} \sin\frac{\pi l}{a} y \sin\frac{\pi l}{a} y' \sinh\frac{\pi l}{a} x_< \sinh\frac{\pi l}{a}(a - x_>). \tag{5.99}$$

This series converges much more rapidly than that of Eq. (5.96), and only a single expansion index is needed.

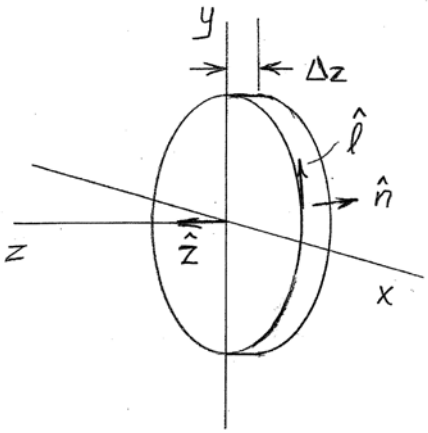

Evaluating the 2D "volume" integral is straightforward, but the "surface" term is less so. To resolve potential ambiguities, we consider the general case. The diagram shows a 3D cylindrical object with end caps at $z = 0$ and $z = \Delta z$. The normal vector $\hat{n}$ to the band connecting the two end caps is everywhere perpendicular to the *z* axis, and the end caps are perpendicular to *z*. By assumption, none of the quantities involved have any *z* dependence. Everything is a function only of $\vec{r}_t$, the two transverse coordinates perpendicular to the *z* axis.

Starting with Green's Theorem,

$$\int_V d^3r' \left(\phi \nabla^2 G(\vec{r},\vec{r}') - G(\vec{r},\vec{r}')\nabla^2\phi\right) = \int_S d^2r' \left(\phi \hat{n}'\cdot\nabla G - G\hat{n}'\cdot\nabla\phi\right), \tag{5.100}$$

we define the Green function by

$$\nabla^2_{\vec{r}} G(\vec{r},\vec{r}') = \nabla^2_{\vec{r}'} G(\vec{r},\vec{r}') = -4\pi\delta(\vec{r}_t - \vec{r}_t'), \tag{5.101}$$

which, as noted above, is dimensionless.

Next, consider integration. The end plates contribute nothing to the surface integral because their mathematical values are equal but their normal vectors point in opposite directions. Since there is no *z* dependence, the band is defined by its intersection with either of the end plates. Let this curve be *C*, with any point on *C* defined by a distance l relative to an index point. The direction of increasing l is determined by the right-hand rule: with the thumb in the direction of the *z* axis, the fingers point in the direction of increasing *l*. If the perimeter is circular, this corresponds to the direction of increasing φ. Now break up d^3r' into $d^3r' = d^2r_t' dz'$ and d^2r' into $d^2r' = dl' dz'$ where dl' is an element along *C*. With no *z* dependences, the z' integration is trivial, yielding Δz throughout. Cancelling this common factor yields

$$\int_S d^2r_t' \left(\phi \nabla_t^2 G(\vec{r}_t,\vec{r}_t') - G(\vec{r}_t,\vec{r}_t')\nabla_t^2\phi\right) = \oint_C dl \left(\phi \hat{n}'\cdot\nabla_t G - G\hat{n}'\cdot\nabla_t\phi\right) \tag{5.102}$$

where *S* is either of the end caps and *C* the path defined above. With *C* defined this way, an elemental area $dA = \frac{dC}{dl} dl\, \Delta z$ of the band along the path is positive definite, consistent with the definition of area.

Substituting the defining equation for *G* in the above gives

$$-4\pi\phi(\vec{r}_t) - \int_S d^2 r_t' \left(G(\vec{r}_t, \vec{r}_t')\nabla_t^2 \phi\right) = \oint_C dl \left(\phi \hat{n}' \cdot \nabla_t G - G\hat{n}' \cdot \nabla_t \phi\right). \tag{5.103}$$

Now

$$\nabla^2 \phi = -4\pi\rho, \tag{5.104}$$

where ρ is the *volume* charge density. However, even with no *z* dependence, ρ continues to have the dimensions of charge per unit volume. Accordingly, ρ can be interpreted as a collection of line charges of linear density Λ, by analogy to the expression for a point charge *q* in three dimensions. In Cartesian coordinates

$$\rho = q\delta(x - x_q)\delta(y - y_q)\delta(z - z_q) \to \Lambda\delta(x - x_q)\delta(y - y_q). \tag{5.105}$$

Thus Poisson's Equation remains dimensionally consistent. Since Λ is a function of lateral coordinates only, we can continue to use ρ as usually interpreted. Continuing, the final two-dimensional expression is

$$\phi(\vec{r}_t) = \int_S d^2 r_t' \, \rho(\vec{r}_t')G(\vec{r}_t, \vec{r}_t') - \frac{1}{4\pi}\oint_C dl \left(\phi \hat{n}' \cdot \nabla_t G - G\hat{n}' \cdot \nabla_t \phi\right), \tag{5.106}$$

where *G* is defined above. The 3D volume and surface integrals have become surface and line integrals, respectively. There are no loose ends – all quantities are defined.

We can represent the line integral in standard notation by substituting

$$\hat{n}' = \hat{l}' \times \hat{z}, \tag{5.107}$$

where $\hat{l}'$ is the unit vector parallel to *C* at the integration point l'. Then

$$\begin{aligned}\phi(\vec{r}_t) &= \int_S d^2 r_t' \, \rho(\vec{r}_t')G(\vec{r}_t, \vec{r}_t') - \frac{1}{4\pi}\oint_C dl \left(\phi \hat{l}' \times \hat{z} \cdot \nabla_t G + G\hat{l}' \times \hat{z} \cdot \nabla_t \phi\right) \\ &= \int_S d^2 r_t' \, \rho(\vec{r}_t')G(\vec{r}_t, \vec{r}_t') - \frac{1}{4\pi}\oint_C \phi \, d\vec{l}' \cdot \left(\phi \hat{z} \times \nabla_t G + G\hat{z} \times \nabla_t \phi\right).\end{aligned} \tag{5.108}$$

The last integral suggests that it might be worth investigating the implications of Stokes' Theorem. Following up on this, consider Dirichlet boundary conditions with $\phi = V$ constant. Then

$$V\oint_C d\vec{l} \cdot \hat{z} \times \nabla_t G = V\int_S d^2 r' \, \hat{z} \cdot \nabla \times (\hat{z} \times \nabla_t G). \tag{5.109}$$

From the inside front cover of Jackson, and using the facts that $\hat{z}$ is also a constant and *G* has no *z* dependence, we have

$$\begin{aligned}\nabla \times (\hat{z} \times \nabla G) &= \hat{z}\nabla \cdot \nabla G - \nabla G(\nabla \cdot \hat{z}) + (\nabla G \cdot \nabla)\hat{z} - (\hat{z} \cdot \nabla)\nabla G \\ &= \hat{z}\nabla_t^2 G = -4\pi \, \hat{z}\,\delta(\vec{r}_t - \vec{r}_t').\end{aligned} \tag{5.110}$$

Hence the surface term reduces to

$$-\frac{1}{4\pi}(-4\pi V) = V\,, \tag{5.111}$$

which is exactly what we expect for a configuration where the boundary is at the uniform potential *V*.

I. Two-dimensional configurations: conformal mapping.

In his second edition, Jackson solves a two-dimensional problem in Sec. 2.10 with a series that can be summed to an analytic expression. In evaluating the series, he provides enough detail so you should be able to follow it. Because the solution is an analytic function of $z = x + iy$, it provides an opportunity to discuss the two-dimensional situation further, specifically regarding complex variables and conformal mapping. These topics arise in a wide range of contexts. Even if you have never had a formal course in complex variables, and even though I won't hold you responsible for this material on either homework or exams, you should at least that conformal mapping exists, along with some of its basic characteristics.

You all know how to deal with complex numbers. Extending this knowledge to two-dimensional boundary-value problems in electrostatics is straightforward. We start by defining the complex variable $z = x + iy$ and consider an analytic function of *z*, which we write as $W(z) = u + iv = u(x, y) + iv(x, y)$. We separate $W(z)$ into real and imaginary parts $u(x, y)$ and $v(x, y)$, respectively, as written. By "analytic" we mean that $W(z)$ can be differentiated one or more times with respect to *z*. The separation into *u* and *v* generally breaks up the connection between *x* and *y* given by $z = x + iy$. Looking at Jackson's Eq. (2.63), you can see that his solution to the configuration of Fig. 2.10 falls into this category

The key points for electrostatics are as follows.

(1) We define two complex planes: *z* and *W*. The horizontal and vertical axes for *z* are *x* and *y*, respectively. Those for *W* are *u* and *v*, respectively.

(2) $W(z)$ defines a *map*, where a point with coordinates (x, y) in *z*-space appears as a point at coordinates (u, v) in *W*-space.

(3) If we have determined that the scalar potential at the point (x, y) in *z*-space is $\phi(x, y)$, then the *same* value ϕ appears at the point (u, v) in *W*-space.

These properties allow us to take a solution in a particular configuration in *z*-space over to a different and presumably more challenging configuration in *W*-space, if we can find a function $W(z)$ that maps the first configuration onto the second. $W(z)$ is known as a *conformal* map, where "conformal" means that in the mapping process angles (but generally not lengths) are preserved. Thus the orthogonality between equipotential and field lines that is characteristic of the *z*-space solution is maintained in *W*-space, except at singular points where derivatives does not exist.

More generally, we can prove that for any analytic function $W(z) = u(x, y) + iv(x, y)$, the functions $u(x, y)$ and $v(x, y)$ satisfy the two-dimensional Laplace Equation

$$\nabla^2 u(x, y) = \nabla^2 v(x, y) = 0 . \tag{5.112}$$

The proof proceeds as follows. We first calculate

$$\frac{\partial W}{\partial x} = \frac{dW}{dz}\frac{\partial z}{\partial x} = \frac{dW}{dz}$$

$$= \frac{\partial u}{\partial x} + i\frac{\partial v}{\partial x} . \tag{5.113}$$

Next, we calculate

$$\frac{\partial W}{\partial y} = \frac{dW}{dz}\frac{\partial z}{\partial y} = i\frac{dW}{dz}$$

$$= \frac{\partial u}{\partial y} + i\frac{\partial v}{\partial y} \tag{5.114}$$

By multiplying the second set of equations by $-i$ we see that

$$\frac{\partial u}{\partial x} = \frac{\partial v}{\partial y} \text{ and } \frac{\partial u}{\partial y} = -\frac{\partial v}{\partial x} . \tag{5.115}$$

These are known as the *Cauchy relations*. They apply as long as $W(z)$ is analytic, so the derivatives exist.

Continuing, we evaluate

$$\nabla^2 W(z) = \nabla^2 \left(u + iv)\right) = \frac{\partial}{\partial x}\left(\frac{\partial u}{\partial x} + i\frac{\partial v}{\partial x}\right) + \frac{\partial}{\partial y}\left(\frac{\partial u}{\partial y} + i\frac{\partial v}{\partial y}\right) . \tag{5.116}$$

We now use the Cauchy relations to convert each term to a mixed derivative of the form $\partial^2 / \partial x \partial y$. Upon finishing we find

$$\nabla^2 W(z) = \frac{\partial}{\partial x}\left(\frac{\partial v}{\partial y} - i\frac{\partial u}{\partial y}\right) + \frac{\partial}{\partial y}\left(-\frac{\partial v}{\partial x} + i\frac{\partial u}{\partial x}\right)$$

$$= 0 . \tag{5.117}$$

Hence we have proven that the real and imaginary parts of any analytic function $W(z)$ each satisfy the Lorentz equation.

Probably the most useful transformation $W(z)$ is the Schwarz-Christoffel (S-C) transformation, which maps a straight line in *W* space into a polygon in *z* space. For reasons that we won't go into here but are related to satisfying various mathematical constraints, the transformation is expressed starting in *W* space and ending in *z* space. The general proof can be found in any textbook on complex variables, and takes of the order of 5 pages. Consequently, we aren't going to prove it here, but only state the

transformation then indicate how it can be applied to the problem that Jackson solves in Sec. 2.10.

To set the stage, the *w*-plane trajectory, called a *contour*, typically follows the *u* axis starting at $u \to -\infty$ and ending at $u \to +\infty$. On the *u* axis are points $u_1, u_2, u_3, \ldots$, which are real numbers. The Schwarz-Christoffel transformation is

$$z = A\int \frac{dw}{(w-u_1)^{(1-\alpha_1/\pi)}(w-u_2)^{(1-\alpha_2/\pi)}(w-u_3)^{(1-\alpha_3/\pi)}\ldots} + B, \tag{5.118}$$

where *A* and *B* are constants (possibly complex). The function *w*(*z*) is not analytic at the poles, so the contour $-\infty < u < \infty$ is distorted into a small semicircle about each singularity to avoid it. This results in a similar distortion in the *z* plane, but through a smaller angle as a result of the powers of $(w-u_j)$ in the above, A transformation with three poles in the denominator and with $\alpha_1 + \alpha_2 + \alpha_3 = 180^\circ$ maps the interior of a triangle in the *z* plane onto the upper half of the complex *w* plane, with the size of the triangle and its 3 angles depending on the values of α_1, α_2, and α_3, and u_1, u_2, and u_3.

We use the configuration in Jackson's Sec. 2.10 as an example. In this case the configuration to be mapped consists of a strip covering $0 \le x \le a$ and $y \ge 0$ where the boundary has right angles at $(x_1, y_1) = (0,0)$ and $(x_2, y_2) = (a,0)$. Needing two right angles, we write the basic transformation as

$$z = A\int \frac{dw}{(w-1)^{1/2}(w+1)^{1/2}} + B = A\int \frac{dw}{(w^2-1)^{1/2}} + B, \tag{5.119}$$

where we have chosen $u_1 = -1$ and $u_2 = 1$ with the idea of keeping the math simple, and later adjusting scaling factors (possibly complex) to adapt our contour to the actual configuration. Setting *A* = 1 and $B = 0$ with the same idea, we have

$$z = \int \frac{dw}{(w^2-1)^{1/2}} = \cosh^{-1}(w). \tag{5.120}$$

so

$$\begin{aligned} w = u + iv &= \cosh(x+iy) \\ &= \cosh(x)\cos(y) + i\sinh(x)\sin(y). \end{aligned} \tag{5.121}$$

With the mapping function defined, we start by investigating boundaries. For $y = 0$ we obtain $u = \cosh(x)$ and $v = 0$. For $y = \pi$ the boundary is $u = -\cosh(x)$ and $v = 0$. For $x = 0$ we get $u = \cos(y)$ and $v = 0$. Thus

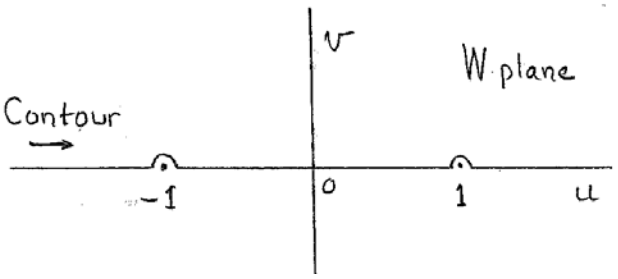

each of the above boundaries in the *z* plane maps onto the *u* axis of the *w* plane, and among them fill it completely over the entire range $-\infty < u < \infty$. These boundaries are illustrated in the figure.

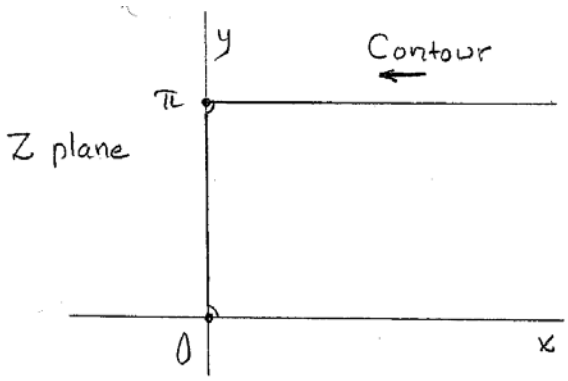

Choosing values of *x* and *y* within these *z*-plane boundaries shows that the *z*-plane region is mapped into the entire upper half of the *w* plane. Conversely, the upper half of the *w* plane is mapped onto the *z*-plane region. Thus we can take our previously obtained *w*-plane solution for $\phi(u,0) = 0$ for $|u| > a$ and $\phi(u,0) = V$ for $|u| \le a$ and map it onto the *z* plane region, To scale and rotate our *z*-plane diagram to conform to that shown in Fig. 2.10 of Jackson, we make the following substitutions: $u_1 \to -\pi/a$, $u_2 \to \pi/a$, $z \to iz$; $x \to \pi x/a$, $y \to \pi y/a$, and $w \to -w$.

Again, the material in this section will not appear in homework assignments or on exams. It is here because you should know that conformal mapping exists.